

nonpolar, exhibiting dipole moments of 0, 0.15, and 0.11, respectively.²¹ Stephany et al. have reported that the ¹³C chemical shift of the isonitrile carbon atom is altered in the presence of water and have attributed this change to hydrogen bonding.²² This also suggests that alkyl isocyanides will be oriented in the micelles with the isonitrile group adjacent to the surface and the alkyl side chain interacting with the hydrocarbon interior. Thus the apparent micellar affinity, K_m' , will be attenuated by a factor representing the extent of partitioning of the isocyno group between the outer hydrated regions of the micelle and the inner hydrocarbon core. Again, it should be emphasized that similar phenomena occur in the case of ligand binding to proteins. The polar isonitriles behave as weak amphipaths and are stabilized near the surface whereas the apolar diatomic ligands exhibit a more uniform concentration gradient throughout the protein structure.

Conclusion

Regardless of the exact mechanistic details, it is clear that the isonitriles react intrinsically more rapidly with heme iron than any of the smaller gaseous ligands (Table I, benzene results). The most plausible explanation of this result is that the polar nature of the isocyno group facilitates the bimolecular binding process. The magnitude of the dipole moment of these ligand molecules indicates a partial negative charge of about $-0.7 e$ on the terminal carbon atom. This value coupled with the partial positive charge on the iron atom suggests that electrostatic considerations alone

(22) Stephany, R. W.; deBie, M. J. A.; Drenth, W. *Magn. Reson.* 1974, 6, 45-47.

could easily account for the 30-fold increase in the observed association rate in going from carbon monoxide to methyl isocyanide. This is particularly true when the reactions are carried out in benzene, which has a very low dielectric constant. In the case of heme dissolved in soap solutions, this favorable effect of the dipole moment is attenuated by stabilization of the polar isocyno group in the outer hydrated regions of the micelle structure. As a result, the bimolecular rate constant for isonitrile binding within the micellar phase, k_m' in eq 6, is more nearly equal to that observed for carbon monoxide binding (Table I).

Acknowledgment. This research was supported by U.S. Public Health Service Grant HL-16093 (J.S.O.), by Grant C612 from the Robert A. Welch Foundation (J.S.O.), by a Teacher-Scholar Award from the Camille and Henry Dreyfus Foundation (J.S.O.), and by a Grant in Aid of Research from Sigma Xi, the Scientific Research Society (D.K.W.). R.E.M. and M.P.M. are recipients of graduate fellowships from the National Institutes of Health Training Grant GM-07833, the National Institute of Medical Science and from the Robert A. Welch Foundation, respectively.

Registry No. Protoheme mono-3-(1-imidazolyl)propylamide mono-methyl ester, 72177-42-5; sodium dodecyl sulfate, 151-21-3; dodecyltrimethylammonium bromide, 1119-94-4; myristyltrimethylammonium bromide, 1119-97-7; cetyltrimethylammonium bromide, 57-09-0; methyl isocyanide, 593-75-9; ethyl isocyanide, 624-79-3; *n*-propyl isocyanide, 627-36-1; *n*-butyl isocyanide, 2769-64-4; *n*-amyl isocyanide, 18971-59-0; *n*-hexyl isocyanide, 15586-23-9; isopropyl isocyanide, 598-45-8; *tert*-butyl isocyanide, 7188-38-7; isobutyl isocyanide, 590-94-3; *sec*-butyl isocyanide, 14069-89-7; cyclohexyl isocyanide, 931-53-3; benzyl isocyanide, 10340-91-7; CO, 630-08-0.

Applications of Molybdenum-95 NMR Spectroscopy. 7.[†] Studies of Metal-Metal Bonded Systems Including Aqueous Molybdenum(IV) and Molybdenum(V). Crystal and Molecular Structure of $\text{Na}_2[\text{Mo}_3\text{O}_4((\text{O}_2\text{CCH}_2)_2\text{NCH}_3)_3]\cdot 7\text{H}_2\text{O}$

Stephen F. Gheller,^{1a} Trevor W. Hambley,^{1b} Robert T. C. Brownlee,^{1a}
Maxwell J. O'Connor,^{*1a} Michael R. Snow,^{1b} and Anthony G. Wedd^{*1a}

Contribution from the Department of Chemistry, La Trobe University, Bundoora, Victoria, 3083, Australia, and the Department of Physical and Inorganic Chemistry, University of Adelaide, Adelaide, South Australia, 5001, Australia. Received May 13, 1982

Abstract: Solution ⁹⁵Mo NMR studies are reported on spin-coupled polynuclear systems of Mo(V), Mo(IV), and Mo(II). Resonances occur at low fields compared to mononuclear species. The chemical shifts of the Mo(IV)-aquo ion in 4 M *p*-toluenesulfonic and methanesulfonic acid media and those of the Mo(IV) complexes containing oxalate, EDTA, and methyliminodiacetate ligands (whose solid-state structures are based on the $[\text{Mo}_3\text{O}_4]^{4+}$ cluster) fall in the narrow range of 172 ppm spanning 990-1162 ppm. As the known chemical shift scale for the ⁹⁵Mo nucleus covers 7000 ppm, this observation indicates that the ⁹⁵Mo nucleus is in a similar chemical environment in each of the species examined and, taken with published evidence, confirms formulation of the Mo(IV)-aquo ion as $[\text{Mo}_3\text{O}_4(\text{H}_2\text{O})_9]^{4+}$. Two resonances are detected in the above range for Mo(IV)_{aq} in 4 M hydrochloric acid and for $[(\text{Mo}_3\text{O}_4)_2(\text{PDTA})_3]^{4-}$. Additional resonances appear at 539-608 ppm in the methanesulfonic acid, hydrochloric acid, and EDTA systems when stored in air. These are assigned to $[\text{Mo}^{\text{V}}_2\text{O}_4]^{2+}$ -based species by comparison with the observed resonances of the Mo(V)-aquo ion, $[\text{Mo}^{\text{V}}_2\text{O}_4(\text{H}_2\text{O})_6]^{2+}$, in the relevant acid media and with $[\text{Mo}^{\text{V}}_2\text{O}_4(\text{EDTA})]^{2-}$ in H₂O. The $[\text{Mo}^{\text{V}}_2\text{O}_4(\text{PDTA})]^{2-}$ anion exhibits two resonances associated with inequivalent molybdenum sites. Resonances for $[\text{Mo}^{\text{II}}_2(\text{O}_2\text{CR})_4]$ (R = CF₃, *n*-Pr), which contain formal quadruple bonds, have been observed for the first time and are the most deshielded ⁹⁵Mo NMR signals detected to date. The methyliminodiacetate complex, $\text{Na}_2[\text{Mo}_3\text{O}_4((\text{O}_2\text{CCH}_2)_2\text{NCH}_3)_3]\cdot 7\text{H}_2\text{O}$, was isolated. Its crystal structure contains a discrete trinuclear $[\text{Mo}^{\text{IV}}_3\text{O}_4((\text{O}_2\text{CCH}_2)_2\text{NCH}_3)_3]^{2-}$ anion whose symmetry approaches C_{3v} and which is closely related to the equivalent trinuclear units connected by EDTA groups that occur in $\text{Na}_4[(\text{Mo}_3\text{O}_4)_2(\text{EDTA})_3]\cdot 14\text{H}_2\text{O}$. Crystal data: monoclinic space group $P2_1/n$; $a = 14.712$ (9) Å, $b = 13.919$ (2) Å, $c = 15.458$ (3) Å, $\beta = 99.80$ (3)°, $V = 3119$ Å³, $Z = 4$.

The nature of the Mo(IV)-aquo ion, Mo(IV)_{aq}, has excited a lively interest since the first demonstrations² of its stability in acid

solution. On the basis of indirect physical and chemical techniques, the structure of Mo(IV)_{aq} was suggested variously to be mono-

[†] For parts 6 and 8, see ref 21i and 21r.

(1) (a) La Trobe University. (b) University of Adelaide.

nuclear^{2a,b,3} or binuclear.^{2c,4} The structurally more sensitive technique of X-ray absorption spectroscopy⁵ ruled out both a mononuclear structure and the presence of terminal oxo ligands, and the binuclear alternative was favored. Unfortunately, the medium used in this study was 4 M HCl, where there is chemical evidence⁶ of a concentration-dependent equilibrium. In addition, there remains the intriguing point that complexes which have been both derived from Mo(IV)_{aq} and structurally characterized in the solid state⁷ are invariably trinuclear species based upon the [Mo₃O₄]⁴⁺ cluster. In fact, 50 years ago, Wardlaw⁸ suggested that the oxalate complex^{7a} was trinuclear. Recent ¹⁸O transfer experiments⁹ in the Mo(IV)_{aq}-NCS⁻ system show that oxo ligands in the inner coordination sphere of Mo(IV)_{aq} are transferred reversibly, and without exchange with solvent water, to the [Mo₃O₄(NCS)₉]⁵⁻ anion. In addition, redox experiments¹⁰ with Mo(IV)_{aq} solutions are convincingly interpreted in terms of trinuclear species. The present work demonstrates the close relationship between the structure of Mo(IV)_{aq} and those of certain trinuclear Mo(IV) complexes in solution and represents the first significant application of ⁹⁵Mo NMR spectroscopy to a structural problem.

In the course of this study, ⁹⁵Mo NMR signals from other spin-coupled systems were observed, namely from [Mo^V₂O₄(H₂O)₉]²⁺ ("Mo(V)_{aq}") and related complexes and from [Mo^{II}₂(O₂CR)₄] (R = CF₃, *n*-Pr).

Experimental Section

Preparation of Solutions of [Mo^{IV}₃O₄(H₂O)₉]⁴⁺. Two-thirds of a solution of Na₆[Mo₇O₂₄]·4H₂O (0.01 M in Mo) in 1 M HPTS¹¹ was reduced with zinc to Mo(III) in a Jones reductor¹² and combined with the remaining one-third volume. The solution was heated at 90 °C under an atmosphere of dinitrogen and purified by cation-exchange chromatography using Dowex 50X-2 resin.^{2c} A sample enriched in ⁹⁵Mo was prepared by using Na₆[Mo₇O₂₄]·4H₂O synthesized¹³ from MoO₃ (96.47 atom % ⁹⁵Mo) purchased from the Oak Ridge National Laboratory. The [⁹⁵Mo₃O₄(H₂O)₉]⁴⁺ ion was transferred to 4 M HMS¹¹ and then 4 M HCl media by (i) initial dilution of the solution to 0.5 M in acid and adsorption of [⁹⁵Mo₃O₄(H₂O)₉]⁴⁺ onto a cation-exchange column, (ii) copious washing of the column with deionized, distilled water, (iii) washing with the replacement acid (1 M) to remove Mo(III) and Mo(V) impurities, and (iv) elution with 4 M acid.

Synthesis of Na₂[Mo₃O₄(C₂O₄)₃(H₂O)₃]·4H₂O. Methyliminodiacetic acid (2.94 g, 20 mmol) was dissolved in NaOH solution (1.6 g, 40 mmol in 6 cm³). This was added to a solution of Mo(IV) (ca. 20 mmol in 25 cm³) eluted from an ion-exchange column with acetate buffer solution (acetic acid (1 M), sodium acetate (1 M)); a sharper band profile results if the buffer is allowed to equilibrate with the column for 1 h before elution). Red crystals are formed by slow evaporation at room temperature. When dry and left open to the atmosphere, the crystals shatter, apparently due to loss of water of crystallization, as indicated by microanalysis. Anal. Calcd for C₁₅H₃₅Mo₃N₃Na₂O₂₃: C, 18.78; H, 3.68; N, 4.38; O, 38.36. Found: C, 19.04, H, 3.11; N, 4.34, O, 34.78.

Cs₂[Mo₃O₄(C₂O₄)₃(H₂O)₃]·4H₂O·0.5H₂C₂O₄ and Na₄[(Mo₃O₄)₂-

Table I. Crystallographic Data

formula	C ₁₅ H ₃₅ Mo ₃ N ₃ Na ₂ O ₂₃
<i>M_r</i>	959.3
<i>a</i> , Å	14.712 (9)
<i>b</i> , Å	13.919 (2)
<i>c</i> , Å	15.458 (3)
β, deg	99.80 (3)
<i>d</i> _{measd} , g cm ⁻³	2.06 (2)
<i>d</i> _{calcd} , g cm ⁻³	2.043
<i>V</i> , Å ³	3119
<i>Z</i>	4
space group	<i>P</i> 2 ₁ / <i>n</i>
μ(Mo Kα), cm ⁻¹	12.70
λ(Mo Kα), Å	0.7107
<i>F</i> (000)	1912
no. of reflectns measd	3996
no. of reflectns used	2868
<i>R</i>	0.037
<i>R_w</i>	0.044

(EDTA)₃·14H₂O¹¹ were prepared by scaling up literature methods.^{7a,b} The new compound Na₄[(Mo₃O₄)₂(PDTA)₃]·14H₂O¹¹ was prepared analogously.^{7b} It was very slow to crystallize (ca. 16 weeks).

Preparation of Solutions of [Mo^V₂O₄(H₂O)₆]²⁺. Details for the preparation of solutions in various acid media have been given previously.¹⁴ In the present work, (pyH)₂[MoOCl₅]¹⁵ was dissolved in 0.1 M HMS or HCl and the solution applied to a Dowex 50X-2 ion-exchange column. The column was copiously washed with deionized, distilled water and with 0.1 M acid before elution with acid of the required strength (1–10 M).

Na₂[Mo₂O₄(EDTA)]·H₂O,^{14b} Na₂[Mo₂O₄(PDTA)]·4H₂O,^{16a} and Na₂[Mo₂O₄(L-cyst)₂]·5H₂O^{15b} were literature preparations. Na₂[Mo₂O₄(L-cyst)₂]·4H₂O^{16c} and Na₂[Mo₂O₄(EDTA)]·2H₂O^{16c} can be conveniently prepared by reduction of a 1:1 mixture of (NH₄)₂[MoO₂S₂] and Na₂[MoO₄]·2H₂O by dithionite in water followed by addition of ligand.

Samples of [Mo₂(O₂CR)₄] (R = CF₃, *n*-Pr) were gifts from Drs. A. F. Masters and K. Cavell. Solutions were generated under strictly anaerobic, anhydrous conditions.

Physical Measurements. Electronic spectra were obtained in matched quartz cells on a Varian Series 634 spectrophotometer.

⁹⁵Mo NMR spectra were recorded at ca. 13.0 MHz, using the pulsed FT NMR technique on a JEOL FX-200 NMR spectrometer. The field homogeneity was adjusted by shimming on the ²H resonance of ²H₂O in a solution of Na₂MoO₄ (2 M) of apparent pH 11.0. Spectral data were collected in the unlocked mode and chemical shifts were referenced externally, using the sample replacement method to the above solution for which $\bar{\nu} = 6516926 (\pm 5)$ Hz at 20 °C. The natural linewidth for a single pulse using 16 384 data points and a spectral bandwidth of 1000 Hz for the standard molybdate solution was 0.6 Hz and the signal to noise ratio was ca. 75:1. Chemical shifts were calculated in parts per million with positive values in the low-field direction relative to the reference. The errors associated in measuring the chemical shift values are ± 1 ppm for line widths <200 Hz, ± 3 ppm for line widths in the range 200–500 Hz, and ± 8 ppm for line widths >500 Hz. The line widths at half-signal height (*W*_{h/2}) reported here have been corrected for exponential line broadening. The error in measuring line widths is ± 5 Hz for line widths <100 Hz, ± 20 Hz for line widths between 100 and 400 Hz, and ± 60 Hz for line widths in excess of 400 Hz.

Spectra were obtained with cylindrical 15-mm o.d. sample tubes (6–8 cm³ sample volume) which were not rotated. Digital spectrometer resolution varied between 2.4 and 4.9 Hz/data point (for 4096 data points), depending on the spectral bandwidth used. Typical acquisition parameters employed in the present systems are given in the captions of Figure 3 and 4. The distorted line shape sometimes observed for overlapping peaks (e.g., Figure 4a) is a consequence of the large phase variation across the spectrum as a result of the delay time imposed prior to data

(2) (a) Souchay, P.; Cadiot, M.; Duhamaux, M. C. *R. Hebd. Seances Acad. Sci.* **1966**, *262*, 1524. (b) Souchay, P.; Cadiot, M.; Viossat, B. *Bull. Soc. Chim. Fr.* **1970**, *3*, 892–896. (c) Ardon, M.; Pernick, A. *J. Am. Chem. Soc.* **1973**, *95*, 6871–6872.

(3) Ramasami, Th.; Taylor, R. S.; Sykes, A. G. *J. Am. Chem. Soc.* **1975**, *97*, 5198–5920.

(4) Ardon, M.; Bino, A.; Yahav, G. *J. Am. Chem. Soc.* **1976**, *98*, 2338–2339.

(5) Cramer, S. P.; Gray, H. B.; Dori, Z.; Bino, A. *J. Am. Chem. Soc.* **1979**, *101*, 2770–2772.

(6) Souchay, P. *J. Inorg. Nucl. Chem.* **1975**, *37*, 1307–1308.

(7) (a) Bino, A.; Cotton, F. A.; Dori, Z. *J. Am. Chem. Soc.* **1978**, *100*, 5252–5253. (b) Bino, A.; Cotton, F. A.; Dori, Z. *Ibid.* **1979**, *101*, 3842–3847.

(c) Murmann, R. K.; Hussain, M. S.; Schlemper, E. O., work quoted in ref 9. (d) Muller, A.; Ruck, A.; Dartmann, M.; Reinsch-Vogell, U. *Angew. Chem., Int. Ed. Engl.* **1981**, *20*, 483–484.

(8) Spittle, H. M.; Wardlaw, W. *J. Chem. Soc.* **1929**, 792–799.

(9) Murmann, R. K.; Shelton, M. E. *J. Am. Chem. Soc.* **1980**, *102*, 3984–3985.

(10) Richens, D. T.; Sykes, A. G. *Inorg. Chem.* **1982**, *21*, 418–422.

(11) Abbreviations: HPTS, *p*-toluenesulfonic acid; HMS, methanesulfonic acid; H₄EDTA, ethylenediaminetetraacetic acid; H₄PDTA, (R,S)-1,2-propylenediaminetetraacetic acid.

(12) Ardon, M.; Pernick, A. *Inorg. Chem.* **1974**, *13*, 2275–2277.

(13) Filowitz, M.; Ho, R. K. C.; Klemperer, W. G.; Shum, W. *Inorg. Chem.* **1979**, *18*, 93–103.

(14) (a) Ardon, M.; Pernick, A. *Inorg. Chem.* **1973**, *12*, 2484–2485. (b) Sasaki, Y.; Sykes, A. G. *J. Chem. Soc., Dalton Trans.* **1974**, 1468–1473. (c) Sasaki, Y.; Taylor, R. S.; Sykes, A. G. *Ibid.* **1975**, 396–400. (d) Cayley, G. R.; Sykes, A. G. *Inorg. Chem.* **1976**, *15*, 2882–2885. (e) Cayley, G. R.; Taylor, R. S.; Wharton, R. K.; Sykes, A. G. *Ibid.* **1977**, *16*, 1377–1381.

(15) Hanson, G. R.; Brunette, A. A.; McDonnell, A. C.; Murray, K. S.; Wedd, A. G. *J. Am. Chem. Soc.* **1981**, *103*, 1953–1959.

(16) (a) Suzuki, K. Z.; Sasaki, Y.; Ooi, S.; Saito, K. *Bull. Chem. Soc. Jpn.* **1980**, *53*, 1288–1298. (b) Kay, A.; Mitchell, P. C. H. *J. Chem. Soc. A* **1970**, 2421–2428. (c) Ott, V. R.; Swieter, D. S.; Schultz, F. A. *Inorg. Chem.* **1977**, *16*, 2538–2545.

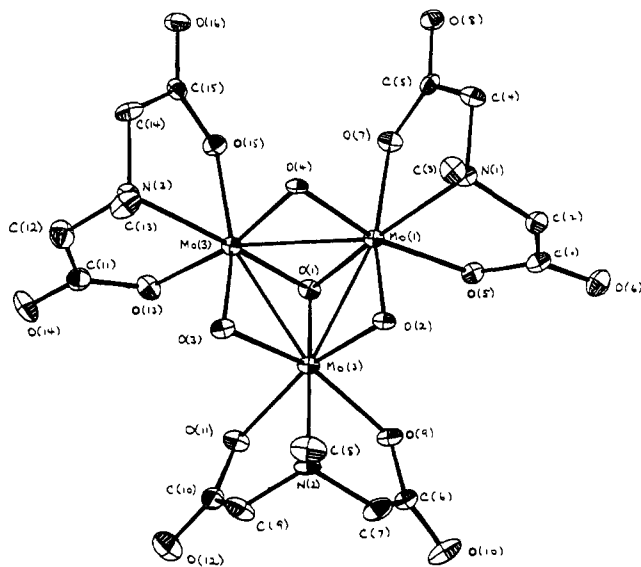


Figure 1. ORTEP diagram of the $[\text{Mo}_3\text{O}_4((\text{O}_2\text{CCH}_2)_2\text{NCH}_3)_3]^{2-}$ anion with atoms drawn as 50% probability ellipsoids viewed down the pseudo- C_3 axis.

accumulation. This delay time is chosen to avoid a rolling base line and was 500–750 μs in the present work.

X-ray Crystallography. A crystal and a small drop of water were sealed in a Lindemann tube. Preliminary precession photographs indicated the monoclinic system while the absences $k = 2n$ for $0k0$ and $h + l = 2n$ for $h0l$ give the space group as $P2_1/n$. Lattice parameters at 23° were determined by a least-squares fit to the setting parameters of 25 independent reflections measured and refined by scans performed on an Enraf-Nonius CAD4 four-circle diffractometer employing graphite monochromated Mo $K\alpha$ radiation. Crystal data is given in Table I.

Intensity data were collected in the range $1.5 < \theta < 22^\circ$, using a $\omega - (n/3)\theta$ scan, where n , optimized by peak analysis, was 4. The ω scan angles and horizontal counter apertures employed were $(1.50 + 0.35 \tan \theta)^\circ$ and $(3.00 + 0.5 \tan \theta)$ mm, respectively. Data reduction and application of Lorentz and polarization corrections were carried out with program SUSCAD.¹⁷ Absorption corrections were not applied.

The positions of the three molybdenum atoms were determined by using the centrosymmetric direct methods routines of the SHELX¹⁸ system of programs. Positions of all other non-hydrogen atoms were obtained from difference maps phased on the three heavy atom positions. Anisotropic refinement of all atoms and calculation of a further difference map revealed all hydrogen atoms in reasonable positions. These were subsequently included, at sites assuming tetrahedral geometry about carbon (C–H 0.97 Å) and with fixed bond lengths (O–H 0.87 Å) and H...H distances (1.41 Å) for the water molecules. Additional electron density was observed in the vicinity of three of the water molecules (O(18), O(19), and O(22)) and was included as a partial occupancy water molecule, complementary to the presence of these water molecules. It is likely that these three water molecules are those lost on exposure of the crystals to the atmosphere. The group multiplicity parameter refined to 0.88 (1).

Blocked-matrix least-squares techniques were used to refine all positional and thermal parameters, using an overall scale factor and an empirical isotropic extinction function of the form $F_o = F_o(1 - 0.0001x F_o^2)/\sin \theta$, where x refined to 0.00002. A weighting scheme was also applied and refined, converging at $w = 0.29/(\sigma^2 F_o + 0.0057 F_o^2)$. A final difference map was structurally featureless with the largest peaks, ca. 1.0 Å⁻³, located in the vicinity of a molybdenum atom. All calculations were performed with the SHELX¹⁸ system of programs and all scattering factors (neutral Mo for Mo(IV)) and anomalous dispersion terms were taken from ref 19.

Results

Crystal Structure. A crystal structure of $\text{Na}_2[\text{Mo}_3\text{O}_4((\text{O}_2\text{CC}-\text{H}_2)_2\text{NCH}_3)_3] \cdot 7\text{H}_2\text{O}$ was necessary to define its stoichiometry as

Table II. Selected Bond Distances (Å) and Angles (deg) for $\text{Na}_2[\text{Mo}_3\text{O}_4((\text{O}_2\text{CCH}_2)_2\text{NCH}_3)_3] \cdot 7\text{H}_2\text{O}$

Bond Distances			
Mo(1)–Mo(2)	2.500 (1)	Mo(2)–O(3)	1.900 (4)
Mo(1)–Mo(3)	2.484 (1)	Mo(2)–O(9)	2.091 (4)
Mo(1)–O(1)	2.031 (4)	Mo(2)–O(11)	2.100 (4)
Mo(1)–O(2)	1.920 (4)	Mo(2)–N(2)	2.238 (5)
Mo(1)–O(4)	1.924 (4)	Mo(3)–O(1)	2.024 (4)
Mo(1)–O(5)	2.050 (4)	Mo(3)–O(3)	1.928 (4)
Mo(1)–O(7)	2.114 (4)	Mo(3)–O(4)	1.925 (4)
Mo(1)–N(1)	2.229 (5)	Mo(3)–O(13)	2.081 (4)
Mo(2)–Mo(3)	2.502 (1)	Mo(3)–O(15)	2.101 (4)
Mo(2)–O(1)	2.073 (4)	Mo(3)–N(3)	2.227 (4)
Mo(2)–O(2)	1.912 (4)		
Bond Angles			
Mo(2)–Mo(1)–Mo(3)	60.3	O(2)–Mo(2)–O(11)	163.6 (2)
O(1)–Mo(1)–O(2)	101.6 (2)	O(2)–Mo(2)–N(2)	86.5 (2)
O(1)–Mo(1)–O(4)	101.2 (2)	O(3)–Mo(2)–O(9)	165.3 (2)
O(1)–Mo(1)–O(5)	86.9 (2)	O(3)–Mo(2)–O(11)	92.7 (2)
O(1)–Mo(1)–O(7)	93.3 (2)	O(3)–Mo(2)–N(2)	88.3 (2)
O(1)–Mo(1)–N(1)	164.4 (2)	O(9)–Mo(2)–O(11)	79.3 (2)
O(2)–Mo(1)–O(4)	94.2 (2)	O(9)–Mo(2)–N(2)	78.2 (2)
O(2)–Mo(1)–O(5)	94.4 (2)	O(11)–Mo(2)–N(2)	79.4 (2)
O(2)–Mo(1)–O(7)	164.6 (2)	Mo(1)–Mo(3)–Mo(2)	60.2
O(2)–Mo(1)–N(1)	87.8 (2)	O(1)–Mo(3)–O(3)	101.1 (2)
O(4)–Mo(1)–O(5)	166.8 (2)	O(1)–Mo(3)–O(4)	107.4 (2)
O(4)–Mo(1)–O(7)	86.7 (2)	O(1)–Mo(3)–O(13)	89.1 (1)
O(4)–Mo(1)–N(1)	90.4 (2)	O(1)–Mo(3)–O(15)	90.8 (2)
O(5)–Mo(1)–O(7)	82.4 (2)	O(1)–Mo(3)–N(3)	164.6 (2)
O(5)–Mo(1)–N(1)	79.9 (2)	O(3)–Mo(3)–O(4)	94.2 (2)
O(7)–Mo(1)–N(1)	76.8 (2)	O(3)–Mo(3)–O(13)	91.9 (2)
Mo(1)–Mo(2)–Mo(3)	59.5	O(3)–Mo(3)–O(15)	166.0 (2)
O(1)–Mo(2)–O(3)	100.4 (2)	O(3)–Mo(3)–N(3)	88.3 (2)
O(1)–Mo(2)–O(9)	94.9 (1)	O(4)–Mo(3)–O(13)	166.6 (2)
O(1)–Mo(2)–O(11)	92.4 (2)	O(4)–Mo(3)–O(15)	90.4 (2)
O(1)–Mo(2)–N(2)	92.3 (2)	O(4)–Mo(3)–N(3)	90.0 (2)
O(1)–Mo(2)–N(2)	168.4 (2)	O(13)–Mo(3)–O(15)	80.9 (2)
O(2)–Mo(2)–O(3)	95.2 (2)	O(13)–Mo(3)–N(3)	78.3 (2)
O(2)–Mo(2)–O(9)	89.7 (2)	O(15)–Mo(3)–N(3)	78.6 (2)

crystals easily lose waters of crystallization. The complex anions, sodium cations, and water molecules participate in an extended hydrogen-bonding network.

The symmetry of the $[\text{Mo}_3\text{O}_4((\text{O}_2\text{CCH}_2)_2\text{NCH}_3)_3]^{2-}$ anion approaches C_{3v} (Figure 1, atomic numbering scheme) and the anion is closely related to the $[\text{Mo}_3\text{O}_4((\text{O}_2\text{CCH}_2)_2\text{NCH}_2)_3]^{2-}$ units in $\text{Na}_4[\text{Mo}_6\text{O}_8(\text{EDTA})_3] \cdot 14\text{H}_2\text{O}$, where two of these units are connected by the ethylene bridges of the three EDTA ligands.^{7b} In both cases, the three nitrogen ligand atoms occupy the δ positions^{7b} cis to the μ_2 bridging atoms (O(2), O(3), O(4)) of the Mo_3O_4 cluster while the six carboxylate oxygen atoms occupy the γ positions cis to the μ_3 bridging atom O(1). Bond distances and angles are very similar in the two structures, and for this reason, a restricted selection only is tabulated in Table II. Full details, including positional and thermal parameters, bond distances and angles, hydrogen-bonding close contacts, and observed and calculated structure factors are provided in the supplementary material.

Electronic Spectra. Table III lists relevant electronic spectra used for monitoring solution concentrations. The results for $[\text{Mo}_3\text{O}_4(\text{H}_2\text{O})_9]^{4+}$ in 4 HPTS and for $\text{Cs}_2[\text{Mo}_3\text{O}_4(\text{C}_2\text{O}_4)_3(\text{H}_2\text{O})_3] \cdot 4\text{H}_2\text{O} \cdot 0.5\text{H}_2\text{C}_2\text{O}_4$ in H_2O (pH 5.5) confirm literature data.^{2b,c,7a} The oxalate, EDTA, and PDTA complexes of Mo(IV) are stable indefinitely in solution. The absorption maximum of the oxalate complex in saturated oxalic acid solution does not change in the temperature range 21–71 °C. The extinction coefficient decreases slightly and reversibly in this range due to Franck–Condon broadening. The methyliminodiacetate complex shows a progressive loss of absorption intensity, detectable after 0.5 h at 10^{-3} M concentration. While standing in air, $\text{Mo(IV)}_{\text{aq}}$ in 4 M HPTS²⁰ and in 4 M HMS progressively loses intensity over a period of days at about 10% per day. It can be repurified and concentrated by cation-exchange chromatography.

(17) SUSCAD, data reduction program for the CAD4 diffractometer, University of Sydney, 1976.

(18) Sheldrick, G. M. SHELX-76, program for crystal structure determination, University Chemistry Laboratory, Cambridge University, 1976.

(19) "International Tables for X-ray Crystallography"; Kynoch Press: Birmingham, U.K., 1974; Vol. IV, p 99.

(20) Ojo, J. F.; Sasaki, Y.; Taylor, R. S.; Sykes, A. G. *Inorg. Chem.* **1976**, *15*, 1006–1009.

Table III. Electronic Spectra

species	solvent	abs max, nm	extn coeff ^a
Mo(IV) _{aq}	4 M HPTS	505	63
	4 M HMS	505	63
Mo(IV) _{aq} ^b	4 M HCl	525	
Na ₄ [(Mo ^{IV} ₃ O ₄) ₂ (EDTA) ₃] 14H ₂ O	H ₂ O (pH 5.5)	542	130
Na ₄ [(Mo ^{IV} ₃ O ₄) ₂ (PDTA) ₃] 14H ₂ O	H ₂ O (pH 5.5)	544	
Na ₂ [Mo ^{IV} ₃ O ₄ ⁻ (O ₂ CH ₂) ₂ NCH ₃] ₃ ·7H ₂ O	H ₂ O (pH 5.5)	529	108
		421	146
		310 sh	371
Cs ₂ [Mo ^{IV} ₃ O ₄ (C ₂ O ₄) ₃ (H ₂ O) ₃] 4H ₂ O·0.5H ₂ C ₂ O ₄	H ₂ O (pH 5.5)	514	114
	satd oxalic acid	514	119 (21 °C)
			114 (51 °C)
			112 (71 °C)
[Mo ^V ₂ O ₄ (H ₂ O) ₆] ²⁺	4 M HMS	384	52
Mo(V) _{aq} ^b	1 M HCl	387	
	4 M HCl	390	
	6 M HCl	401	

^a Extinction coefficient per equivalent of molybdenum.

^b Spectra of NMR samples at room temperature; see Table IV.

The spectrum of [Mo^V₂O₄(H₂O)₆]²⁺ in 4 M HMS conforms with that reported^{14b} in 0.5–5.0 M HClO₄. The absorption maxima of both Mo(IV)_{aq} and Mo(V)_{aq} in 4 M HCl show bathochromic shifts relative to those observed in 4 M HMS. In fact, for Mo(V)_{aq}, the absorption maximum is dependent on HCl concentration in the range 1–6 M. (Table III).

⁹⁵Mo Nuclear Magnetic Resonance. Chemical shift and line width data are presented in Table IV for the various Mo(V), Mo(IV), and Mo(II) species. Mo(IV)_{aq} solutions were examined at 0.05–0.06 M in molybdenum as previous investigations of this system have usually employed concentrations in the range 0.01–0.1 M. However, signals proved difficult to observe at ambient temperature in these concentrated (4 M) acid solutions of high viscosity but could be observed in the temperature range 50–75 °C for samples enriched to 96.7 atom % in ⁹⁵Mo. The integrity of the solutions was confirmed by electronic spectroscopy at room temperature before and after the NMR measurement. All other systems were examined at natural abundance concentrations of molybdenum of 0.1–1.0 M. The only Mo(IV) system whose NMR signal was observed at ambient temperature was [Mo₃O₄(C₂O₄)₃(H₂O)₃]²⁻. The qualitative features of its electronic (Table III) and ⁹⁵Mo NMR (Table IV) spectra were not temperature dependent in the range 20–75 °C. The reduction of the NMR line width with increasing temperature is attributed to correlation narrowing as the viscosity decreases.

All Mo(V) systems were stable in air for days, but new resonances appear in certain Mo(IV) systems when stored in air. The Mo(IV)-oxalate and -EDTA complexes exhibit resonances at 1041 and 1083 ppm, respectively (Figure 2a). In the EDTA system, another resonance at 608 ppm appears after a few weeks storage in air and is due to the Mo(V) species [Mo^V₂O₄(EDTA)]²⁻ (Table IV). The [Mo^{IV}₃O₄(H₂O)₃]⁴⁺ ion in 4 M HPTS at 50 °C resonates at 1133 ppm. The signal shifts to 990 ppm upon transfer to 4 M HMS (Figure 2b). In this medium, a signal at 539 ppm due to the Mo(V)-aquo ion, [Mo^V₂O₄(H₂O)₆]²⁺, progressively appears after a few weeks. In 4 M HCl, two resonances at 1162 and 1024 ppm are observed initially and a third progressively appears at 550 ppm (Figure 2c). The latter is attributed to [Mo^V₂O₄(H₂O)₆]²⁺ (Table IV). [(Mo^{IV}₃O₄)₂(PDTA)₃]⁴⁻ and [Mo^V₂O₄(PDTA)]²⁻, which both contain the unsymmetrical ligand (*R,S*)-[(O₂CCH₂)₂NCH(CH₃)CH₂N(CH₂CO₂)₂]⁴⁻ show two resonances at δ 1103 and 1025 and at 635 and ca. 590, respectively (Figure 3).

Resonances for binuclear Mo(II) species which contain formal quadruple bonds have been observed for the first time (Table IV).

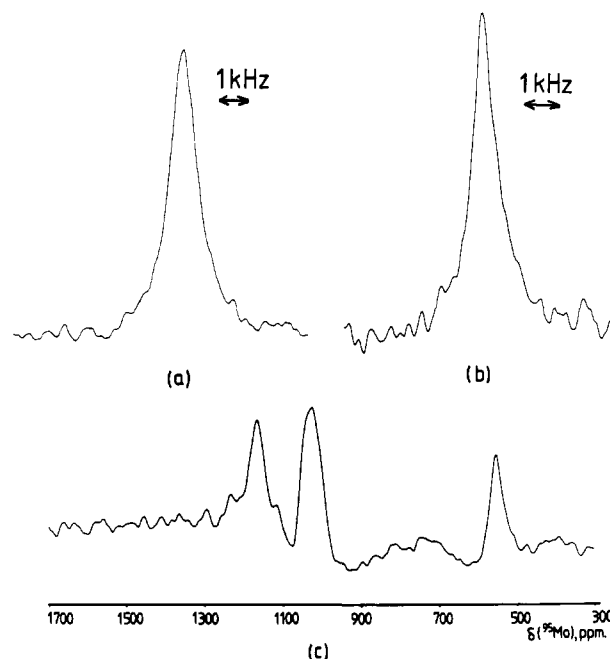


Figure 2. ⁹⁵Mo NMR spectra: (a) Cs₂[Mo₃O₄(C₂O₄)₃(H₂O)₃]₄H₂O·0.5H₂C₂O₄ in saturated oxalic acid solution (number of pulses, 17 000; pulse repetition time, 215 ms; spectral bandwidth, 10 kHz; exponential line broadening, 100 Hz; temperature, 20 °C); (b) Mo(IV)_{aq} in 4 M HMS (96.47 atom % ⁹⁵Mo; number of pulses, 360 000; pulse repetition time, 61.2 ms; spectral bandwidth, 20 kHz; exponential line broadening, 250 Hz; temperature, 50 °C); (c) Mo(IV)_{aq} in 4 M HCl after standing in air for 1 week (96.47 atom % ⁹⁵Mo; number of pulses, 360 000; pulse repetition time, 112.4 ms; spectral bandwidth, 20 kHz; exponential line broadening, 250 Hz; temperature, 50 °C).

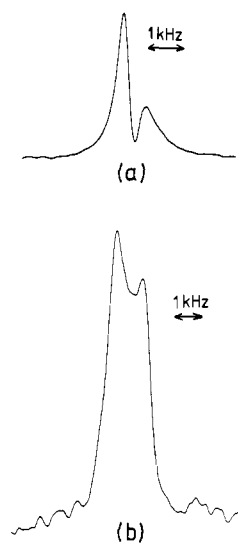


Figure 3. ⁹⁵Mo NMR spectra: (a) Na₂[Mo₂O₄(PDTA)]·4H₂O in H₂O (pH 5.5); see comments in the experimental section concerning the distorted line shapes (number of pulses, 87 000; pulse repetition time, 112.4 ms; spectral bandwidth, 20 kHz; exponential line broadening, 200 Hz; temperature, 70 °C); (b) Na₄[(Mo₃O₄)₂(PDTA)₃]₁₄H₂O in H₂O (pH 5.5) (number of pulses: 330 000; pulse repetition time, 112.4 ms; spectral bandwidth, 20 kHz; exponential line broadening, 250 Hz; temperature, 75 °C).

[Mo^{II}₂(O₂CCF₃)₄] has the most deshielded ⁹⁵Mo NMR signal (4026 ppm) detected to date.

Discussion

A detailed NMR chemical shift scale for the quadrupolar nucleus ⁹⁵Mo (*I* = 5/2; *Q* ~ 0.011 × 10⁻²⁴ cm²; natural abundance, 15.72 atom %) is currently being developed.²¹ With the obser-

Table IV. ⁹⁵Mo NMR Data

species	solvent medium	Mo concn, M	T, °C	δ	W _{H/2} , Hz ^a
Mo(IV) _{aq}	4 M HPTS	0.061 ^b	50	1133	350
	4 M HMS	0.050 ^b	50	990	620
Mo(IV) _{aq}	4 M HCl	~0.05 ^b	50	539 ^c	350
				1162	450
				1024	550
H ₂ [Mo ^{IV} ₃ O ₄ (C ₂ O ₄) ₃ (H ₂ O) ₃]	satd oxalic acid	1.0	20	550 ^c	~500
				1044	520
				1049	260
				1053	170
Na ₄ [(Mo ^{IV} ₃ O ₄) ₂ (EDTA) ₃].14H ₂ O	D ₂ O	0.3	50	1083	1000
				608 ^c	~500
Na ₂ [Mo ^{IV} ₃ O ₄ ((O ₂ CCH ₂) ₂ NCH ₃) ₃].7H ₂ O	H ₂ O (pH 5.5)	0.28	50	1037	250
Na ₄ [(Mo ^{IV} ₃ O ₄) ₂ (PDTA) ₃].14H ₂ O	H ₂ O (pH 5.5)	~0.2	75	1103	1400 ^d
Mo(V) _{aq}	1-6 M HMS	0.13-0.18	20	533	500-670 ^e
			50	542	260-390 ^e
	1-6 M HCl	0.17-0.28	20	535	450
			50	547	230-260 ^e
			50	609	490
Na ₂ [Mo ^V ₂ O ₄ (EDTA)].H ₂ O	H ₂ O (pH 5.5)	0.1	20	609	490
Na ₂ [Mo ^V ₂ O ₄ (PDTA)].4H ₂ O	H ₂ O (pH 5.5)	0.5	70	635	~200 ^d
Na ₂ [Mo ^V ₂ O ₄ (L-cyst) ₂].5H ₂ O	H ₂ O (pH 5.2)	0.1	50	434	250
Na ₂ [Mo ^V ₂ O ₄ (O ₂ S ₂ (EDTA)].2H ₂ O	H ₂ O (pH 5.0)	0.05	50	982	300
Na ₂ [Mo ^V ₂ O ₄ (O ₂ S ₂ (L-cyst) ₂)].4H ₂ O	H ₂ O (pH 6.6)	0.1	50	637	630
[Mo ^{II} (O ₂ Cn-Pr) ₄]	DMF	0.8	70	3730	1400
[Mo ^{II} ₂ (O ₂ CCF ₃) ₄]	THF	1.0	55	4026	250

^a Corrected for exponential line broadening. ^b Enriched to 96.7 atom % ⁹⁵Mo. ^c Appeared in aerobic solutions upon storage of samples in air. ^d Combined width of overlapping resonances (see Figure 4). ^e Increases with increasing acid concentration due to increasing viscosity of the medium.

vation of a resonance at 4026 ppm for [Mo₂(O₂CCF₃)₄] (Table IV), it currently covers 7000 ppm. This extended range, coupled with fast data acquisition permitted by the rapid relaxation rates imposed by quadrupolar relaxation, can compensate substantially for quadrupolar broadening effects. Detection of signals in the present work was enhanced by ⁹⁵Mo enrichment and examination at elevated temperatures to reduce the effects of correlation broadening in the highly viscous acid media employed. For immediate purposes, the following empirical points are relevant:

(a) For mononuclear species, the chemical shift varies with oxidation state in the following way: Mo(VI), 3200 to -200 ppm;^{21a-j} Mo(IV), -300 to -3000 ppm;^{21h,j} Mo(II), -100 to -2072 ppm;^{21j-n} Mo(0), -770 to -2200 ppm.^{21m,o-r} The ranges for oxidation states IV, II, and 0 overlap,^{21r} and the chemical shift is not an independent indicator of oxidation state. The extended ranges follow from the sensitivity of the electronic environment of the metal nucleus in mononuclear complexes to the exact nature of the complexing ligands and, in certain cases, to the solvent (e.g., the solvent dependency of the chemical shift of [MoS₄]²⁻ is over 80 ppm^{21e}). In addition, it is probable that shifts due to weak

paramagnetic effects (e.g., temperature-independent paramagnetism) are affecting the observed resonance positions in some examples.

(b) The chemical shift range^{21d,j} for the polynuclear poly(oxomolybdate(VI)) anions of 110 to -20 ppm is included in the range for mononuclear Mo(VI) compounds, as might be expected for species in which the metal sites interact minimally. However, for polynuclear species of lower oxidation state where covalent interactions between the metals is an accepted feature,²² chemical shifts may fall outside the ranges observed for mononuclear species. Indeed, [Mo^{II}₂(O₂CCF₃)₄] and [Mo^{II}₂(O₂Cn-Pr)₄], with their formal quadruple resonance, resonate at 4026 and 3730 ppm, far removed from the existing range for mononuclear Mo(II) species: -100 to -2072 ppm.

Molybdenum(IV) Systems. The ⁹⁵Mo chemical shift range observed in this work for Mo(IV)_{aq} and the related Mo(IV) complexes (whose trinuclear solid state structures are consistent with the presence of Mo-Mo single bonds²²) is 990-1162 ppm, which can be compared to that presently defined²³ for mononuclear Mo(IV) species: -300 to -3000 ppm. The narrowness of the observed range (172 ppm) is significant. It indicates that the ⁹⁵Mo nucleus is in a similar molecular and electronic environment in all of the Mo(IV) species examined, consistent with the presence of the [Mo^{IV}₃O₄]⁴⁺ cluster, whose internal covalent bonding is relatively unperturbed by change of peripheral ligand and of solvent medium. A recent theoretical analysis^{22b} supports the latter point.

In the 4 M HCl system, two resonances attributable to [Mo₃O₄]⁴⁺ clusters occur (Figure 2c). The conditions of ion-exchange elution of the sample require that the charges on the eluting species be 3+ or greater, but the situation is complicated by the probability of ligand exchange involving H₂O and Cl⁻ (there are three equivalent peripheral sites of one kind and six of another in [Mo₃O₄(H₂O)₉]⁴⁺). At this stage, the simplest interpretation

(21) (a) Vold, R. R.; Vold, R. L. *J. Magn. Reson.* **1975**, *19*, 365-371. (b) Kautt, W. D.; Kruger, H.; Lutz, O.; Maier, H.; Nolle, A. *Z. Naturforsch.* **1976**, *31A*, 351-356. (c) Lutz, O.; Nolle, A.; Kroneck, P. *Ibid.* **1976**, *31A*, 454-456; **1977**, *32A*, 505-506. (d) Masters, A. F.; Gheller, S. F.; Brownlee, R. T. C.; O'Connor, M. J.; Wedd, A. G. *Inorg. Chem.* **1980**, *19*, 3866-3868. (e) Gheller, S. F.; Gazzana, P. A.; Masters, A. F.; Brownlee, R. T. C.; O'Connor, M. J.; Wedd, A. G.; Snow, M. R. *Inorg. Chim. Acta* **1981**, *54*, L131-L132. (f) Christensen, K. A.; Miller, P. E.; Minelli, M.; Rockway, T. W.; Enemark, J. H. *Ibid.* **1981**, *56*, L27-L28. (g) Freeman, M. A.; Schultz, F. A.; Reilly, C. N. *Inorg. Chem.* **1982**, *21*, 567-576. (h) Lee, R. K.; Howlader, N. C.; Haight, G. P.; Oldfield, E., submitted for publication. (i) Gheller, S. F.; Traill, P. R.; Brownlee, R. T. C.; O'Connor, M. J.; Wedd, A. G.; Hampley, T. W.; Snow, M. R. *Aust. J. Chem.* **1982**, *35*, 2183-2191. (j) Gheller, S. F.; O'Connor, M. J.; Wedd, A. G., unpublished observations. (k) Masters, A. F.; Brownlee, R. T. C.; O'Connor, M. J.; Wedd, A. G.; Cotton, J. D. *J. Organomet. Chem.* **1980**, *195*, C17-C20. (l) Brownlee, R. T. C.; Masters, A. F.; O'Connor, M. J.; Wedd, A. G.; Kimlin, H. A.; Cotton, J. D. *Org. Magn. Reson.* **1982**, *20*, 73-77. (m) Dysart, S.; Georgii, I.; Mann, B. E. *J. Organomet. Chem.* **1981**, *213*, C10-C12. (n) LeGall, J. Y.; Kubicki, M. M.; Petillon, F. Y. *Ibid.* **1981**, *221*, 287-290. (o) Masters, A. F.; Brownlee, R. T. C.; O'Connor, M. J.; Wedd, A. G. *Inorg. Chem.* **1981**, *20*, 4183-4186. (p) Minelli, M.; Rockway, T. W.; Enemark, J. H.; Brunner, H.; Muschiol, M. *J. Organomet. Chem.* **1981**, *217*, C34-C35. (q) Bailey, J. T.; Clark, R. J.; Levy, G. C. *Inorg. Chem.* **1982**, *21*, 2085-2087. (r) Masters, A. F.; Bossard, G. E.; George, T. A.; Brownlee, R. T. C.; O'Connor, M. J.; Wedd, A. G. *Inorg. Chem.*, in press.

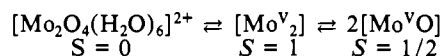
(22) (a) Muller, A.; Jostes, R.; Cotton, F. A. *Angew. Chem., Int. Ed. Engl.* **1980**, *19*, 875-882 and references therein. (b) Bursten, B. E.; Cotton, F. A.; Hall, M. G.; Najjar, R. C. *Inorg. Chem.* **1982**, *21*, 302-307.

(23) Solutions obtained upon dissolution of K₄[MoO₂(CN)₆] and K₂[MoO(OH)(CN)₄] in basic media show ⁹⁵Mo NMR signals at +1400-1500 ppm.²¹ As other Mo(IV) species containing oxo or cyano ligands resonate in the "mononuclear" range (-300 to -3000 ppm), the species responsible for the above resonances may be polynuclear.

is that two members of the equilibrium are being observed, but it is possible that a single species, such as $[\text{Mo}_3\text{O}_4(\text{H}_2\text{O})_8\text{Cl}]^{3+}$ (whose inequivalent Mo sites are interconverting slowly on the ^{95}Mo NMR time scale; vide infra), is contributing. Note that the electronic spectrum differs from that observed for $\text{Mo(IV)}_{\text{aq}}$ in 4 M HMS and HPTS (Table III). An equilibrium dependent upon HCl concentration has been reported,⁶ as has the observation of two bands (one of which contains Cl^-) when Cl^- -containing solutions of Mo(IV) in HPTS are eluted from a cation-exchange column.²⁰ Similar equilibria are postulated^{7b} in Mo(IV) solutions in HF. The present observations may be relevant to interpretation of the EXAFS data⁵ on Mo(IV) in 4 M HCl.

Molybdenum(V) Systems. $\text{Mo(IV)}_{\text{aq}}$ in 4 M HMS and HCl and $[(\text{Mo}_3\text{O}_4)_2(\text{EDTA})_3]^{4-}$ in H_2O undergo slow aerial oxidation to produce Mo(V)_{aq} (Figure 2c) and $[(\text{Mo}_2\text{O}_4)(\text{EDTA})]^{2-}$, respectively. The chemical shift observed for Mo(V)_{aq} is independent of acid concentration in the range 1–6 M for both HMS and HCl, suggesting the presence of $[(\text{Mo}_2\text{O}_4)(\text{H}_2\text{O})_6]^{2+}$ in both systems. However, note that the electronic spectrum of Mo(V)_{aq} is dependent upon HCl concentration (Table III). Solutions of Mo(V)_{aq} in HCl were generated in the present work by two methods: (i) dissolution of $(\text{pyH})_2[\text{MoOCl}_5]$ in 0.1 M acid followed by adsorption onto and elution from a cation-exchange column;¹⁴ (ii) simple dissolution of $(\text{pyH})_2[\text{MoOCl}_5]$ in acid of the required concentration.

In the range 1–4 M HCl the ^{95}Mo NMR signal of Mo(V)_{aq} was observed and the observation was independent of the method of preparation. However, when $[\text{HCl}] \geq 6$ M, a resonance was observed for solution (i) but not for solution (ii), even after 24 h when aequation would certainly be complete.²⁴ Interestingly, detectable concentrations of paramagnetic mononuclear and, apparently, paramagnetic binuclear species appear²⁵ in Mo(V)_{aq} solutions when $[\text{HCl}] > 4$ M:



The above results suggest that the approach to equilibrium via $[(\text{Mo}_2\text{O}_4)(\text{H}_2\text{O})_6]^{2+}$ is slow.

EDTA and PDTA Complexes. $[(\text{Mo}_2\text{O}_4)(\text{EDTA})]^{2-}$ and $[(\text{Mo}_2\text{O}_4)(\text{PDTA})]^{2-}$ exhibit one and two ^{95}Mo NMR resonances, respectively (Figure 3a). The methyl group on the backbone of the PDTA ligand removes the C_2 symmetry axis present in the EDTA complex and allows the possibility of two geometric isomers. One isomer has an "equatorial" methyl group directed away from the plane of the di- μ -oxo bridge while the other has a highly strained "axial" methyl group directed toward this plane. The presence of the equatorial isomer is confirmed²⁶ in the solid state for $\text{Na}_2[(\text{Mo}_2\text{O}_4)(\text{PDTA})] \cdot 3\text{H}_2\text{O}$. ^1H and ^{13}C NMR studies²⁷ show the presence of a single species, suggested to be the equatorial isomer, which is conformationally rigid in the temperature range 0–90 °C. Consequently, the two ^{95}Mo NMR resonances resolved

at 70 °C in $[(\text{Mo}_2\text{O}_4)(\text{PDTA})]^{2-}$ are assigned to resonance on the nonequivalent Mo sites of the equatorial isomer. A similar resolution of nonequivalent sites obtains^{21ij} for the Mo(VI) species $[(\text{MoO}_3)_2(\text{EDTA})]^{2-}$ and $[(\text{MoO}_3)_2(\text{PDTA})]^{2-}$, where, respectively, one and two ^{95}Mo NMR resonances are observed.

$[(\text{Mo}_3\text{O}_4)_2(\text{EDTA})_3]^{4-}$ and $[(\text{Mo}_3\text{O}_4)_2(\text{PDTA})_3]^{4-}$ also exhibit one and two ^{95}Mo NMR resonances, respectively (Figure 3b). The EDTA complex consists^{7b} of equivalent trinuclear units connected by EDTA groups and its symmetry approaches C_{3v} . Substitution by PDTA will lead to inequivalent trinuclear units and two structural isomers: a "symmetrical" isomer with the three methyl groups adjacent to one trinuclear unit and an "unsymmetrical" isomer with two methyl groups adjacent to one trinuclear unit. The methyl substituents in these isomers of $[(\text{Mo}_3\text{O}_4)_2(\text{PDTA})_3]^{4-}$ are unlikely to be as sterically constrained as those in $[(\text{Mo}_2\text{O}_4)(\text{PDTA})]^{2-}$, and the possibility of various conformers and stereoisomers complicate the system. However, the resolution of nonequivalent sites in the Mo(VI) and Mo(V) species suggest a similar assignment for $[(\text{Mo}_3\text{O}_4)_2(\text{PDTA})_3]^{4-}$; i.e., that $\text{Mo} \leftarrow \text{N} \leftarrow \text{CHMe}$ and $\text{Mo} \leftarrow \text{N} \leftarrow \text{CH}_2$ sites are nonequivalent on the ^{95}Mo NMR time scale.

Conclusions

The ^{95}Mo nuclei in the spin-coupled, polynuclear species examined in the present work are highly deshielded compared to mononuclear species. This point is relevant to future applications of ^{95}Mo NMR spectroscopy and probably to certain other transition-metal nuclei as well.

^{95}Mo resonances were detected in solution in the narrow chemical shift range of 990–1162 ppm for $\text{Mo(IV)}_{\text{aq}}$ in various acid media and also for complexes which contain the Mo_3O_4 unit in the solid state (Figure 1 and ref 7). When coupled with the ^{18}O transfer experiments⁹ and the EXAFS evidence,⁵ the results confirm that Mo(IV) solutions in acid media contain high proportions of the $[(\text{Mo}_3\text{O}_4)(\text{H}_2\text{O})_6]^{4+}$ ion and simple complexes derived from it by substitution of water ligands.

Acknowledgment. We thank Professors J. H. Enemark, G. P. Haight, G. C. Levy, and E. Oldfield for preprints of results. The Australian Research Grants Committee and the Australian Wool Corp. are thanked for generous support of this work. The FX-200 spectrometer was purchased from grants from the following: the Vice-Chancellor's Development Fund (La Trobe University), the Sunshine Foundation, the Ian Potter Foundation, BASF Australia Ltd., and the Bank of New South Wales. We gratefully acknowledge these donors and also thank H. A. Holterhoff, JEOL (Australasia) Pty. Ltd., for technical advice and assistance in the establishment of the NMR facility.

Registry No. $[(\text{Mo}_3\text{O}_4)(\text{H}_2\text{O})_6]^{4+}$, 74353-85-8; $\text{Na}_2[(\text{Mo}_3\text{O}_4)(\text{MIDA})_3] \cdot 7\text{H}_2\text{O}$, 84642-29-5; $[(\text{Mo}_2\text{O}_4)(\text{H}_2\text{O})_6]^{2+}$, 52757-71-8; $\text{Na}_4[(\text{Mo}_3\text{O}_4)_2(\text{EDTA})_3]$, 71356-70-2; $\text{Na}_4[(\text{Mo}_3\text{O}_4)_2(\text{PDTA})_3]$ (symmetrical isomer), 84647-87-0; $\text{Na}_4[(\text{Mo}_3\text{O}_4)_2(\text{PDTA})_3]$ (unsymmetrical isomer), 84642-30-8; $\text{Cs}_2[(\text{Mo}_3\text{O}_4)(\text{C}_2\text{O}_4)_3(\text{H}_2\text{O})_3]$, 67620-45-5; $\text{H}_2[(\text{Mo}_3\text{O}_4)(\text{C}_2\text{O}_4)_3(\text{H}_2\text{O})_3]$, 84623-96-1; $\text{Na}_2[(\text{Mo}_2\text{O}_4)(\text{EDTA})]$, 53632-26-1; $\text{Na}_2[(\text{Mo}_2\text{O}_4)(\text{PDTA})]$, 84623-97-2; $\text{Na}_2[(\text{Mo}_2\text{O}_4)(\text{L-cyst})_2]$, 23331-32-0; $\text{Na}_2[(\text{Mo}_2\text{O}_2\text{S}_2)(\text{EDTA})]$, 62569-65-7; $\text{Na}_2[(\text{Mo}_2\text{O}_2\text{S}_2)(\text{L-cyst})_2]$, 29683-41-8; $[(\text{Mo}_2)(\text{O}_2\text{C}-n\text{-Pr})_4]$, 41772-56-9; $[(\text{Mo}_2)(\text{O}_2\text{CCF}_3)_4]$, 36608-07-8; Mo , 7439-98-7; ^{95}Mo , 14392-17-7.

Supplementary Material Available: Full listings of positional and thermal parameters, bond distances and angles, hydrogen-bonding close contacts, and observed and calculated structure factors are contained in Tables S1–S6 (23 pages). Ordering information is given on any current masthead page.

(24) After storage of a sample of solution (ii) in 6 M HCl for 8 weeks, a resonance (δ 153; $W_{h/2}$ 220 Hz) had appeared. This is not due to $[(\text{Mo}_2\text{O}_4)(\text{H}_2\text{O})_6]^{2+}$ (Table IV), and the species responsible is unknown.

(25) (a) Haight, G. P., Jr. *J. Inorg. Nucl. Chem.* **1962**, *24*, 663–667. (b) Hare, C. R.; Bernal, I.; Gray, H. B. *Inorg. Chem.* **1962**, *1*, 831–835. (c) Yoshino, Y.; Taminaga, I.; Uchida, S. *Bull. Chem. Soc. Jpn.* **1971**, *44*, 1435–1437.

(26) (a) Wing, R. M.; Callahan, K. P. *Inorg. Chem.* **1969**, *8*, 2303–2306. (b) Kojima, A.; Ooi, S.; Sasaki, Y.; Suzuki, K. Z.; Saito, K.; Kuroya, H. *Bull. Chem. Soc. Jpn.* **1981**, *54*, 2457–2465.

(27) (a) Haynes, L. V.; Sawyer, D. T. *Inorg. Chem.* **1967**, *6*, 2146–2150. (b) Blackmer, G. L.; Johnson, K. J.; Roberts, R. L. *Ibid.* **1976**, *15*, 596–601.